Light reflector, amplifier, and splitter based on gain-assisted photonic band gaps

Yan Zhang,[1,2] Yi-Mou Liu,[1] Tai-Yu Zheng,[1] and Jin-Hui Wu[1,*]

[1]*School of Physics and Center for Quantum Sciences, Northeast Normal University, Changchun 130024, China*

[2]*Department of Physics and Astronomy, University of Rochester, Rochester, New York 14627, USA*

(Received 21 March 2016; published 19 July 2016)

We study both the steady and the dynamic optical response of cold atoms trapped in an optical lattice and driven to the three-level Λ configuration. These atoms are found to exhibit gain without population inversion when an incoherent pump is applied to activate spontaneously generated coherence. Gain-assisted double photonic band gaps characterized by reflectivities over 100% then grow up near the probe resonance due to the periodic distribution of the atomic density. These band gaps along with the neighboring allowed bands of transmissivities over 100% can be tuned by modulating the control field in amplitude, frequency, and, especially, phase. Consequently it is viable to realize a reflector, an amplifier, or a splitter when a weak incident light pulse is totally reflected in the photonic band gaps, totally transmitted in the allowed bands, or equally reflected and transmitted in the intersecting regions. Our results have potential applications in all-optical networks with respect to fabricating dynamically *switchable* devices for manipulating photon flows at low-light levels.

DOI: 10.1103/PhysRevA.94.013836

I. INTRODUCTION

In recent years, shaping and controlling photon flows with photonic band gaps (PBGs), a key technique for realizing photonic quantum manipulation, has attracted intense research interest [1–4] because of its imminent applications in developing novel photonic devices and circuits [5]. As a kind of naturally or artificially inhomogeneous material, photonic crystals possess periodic modulations of the *real* refractive index, then yielding PBGs close to the Brillouin-zone boundaries in which the light pulses of a range of wave vectors cannot freely propagate owing to multiple Bragg reflections [1,2,6–8]. The control of photon flows with tunable PBGs is often desired for all-optical devices and circuits in communication networks; this is, however, rather difficult or even impossible for photonic crystals of fixed periodic structures [2,4,9]. In this regard, all–optically tunable PBGs have been studied in theory and experiment by exploiting various atomic coherence effects like electromagnetically induced transparency (EIT) [4,10–19]. In a typical EIT-based scheme for generating PBGs, two strong counter-propagating laser fields form a standing-wave pattern and act on the same atomic transition in the absence of, e.g., optical pumping and nonresonant scattering. When they are finely adjusted in terms of amplitude, frequency, and relative angle, narrow PBGs of high reflection could be attained in a small frequency range [20–24] where the *real* (*imaginary*) part of a complex susceptibility referring to *absorption* (*dispersion*) is greatly suppressed (periodically modulated). These schemes are challenging to realize experimentally since rather complicated light-matter interactions are involved, especially for high-order PBGs with short-wavelength signals controlled by long-wavelength standing waves [18,19].

In addition to homogeneous atomic clouds, cold atoms trapped in an optical lattice (OpL) may also be taken as a periodic EIT medium to attain more flexibility in generating all–optically tunable PBGs. An OpL is formed by the interference of two far-detuned counter-propagating laser fields, creating periodic dipole potentials capable of trapping frozen atoms in the wavelength-sized wells [25–29]. This has been extensively studied both experimentally and theoretically, e.g., to generate entanglement in light-atom interfaces [30,31] and simulate transport features of quantum materials [32]. One typical function of atomic arrays in an OpL is to serve as dynamically controlled reflectors because their PBGs can be modulated in positions and widths to yield high reflectivities for incident light pulses [3,33]. This has been observed in the one-dimension case [34–38] and predicted in the three-dimension case [39,40], where at least one traveling-wave laser field is applied to the trapped atoms in a suitable EIT level configuration [41–44]. Similar PBG generation schemes have led to many attractive and significant phenomena, like radiation damping enhancement [45], optical nonreciprocity [45], and optical parity-time symmetry [46,47]. However, reflectivities of such PBGs are usually less than 80% as restricted by the finite optical depths of cold atoms and the residual absorption due to inevitable dephasings [38,42].

Here we try to propose an efficient scheme for manipulating on demand the photon flows of a weak probe field when it travels through a sample of cold atoms trapped in an OpL. The main idea is to realize gain-assisted PBGs [48] by avoiding absorptive loss with spontaneously generated coherence (SGC), an effect referring to the situation, e.g., in which spontaneous decay from an excited-state level results in coherence between two ground-state levels [49–52]. It has been shown that the nontrivial SGC effect can result in interesting phenomena such as spontaneous mission cancelation [53], quantum interference enhancement [54], large self-phase modulation [55], and gain without population inversion [56,57]. Some of these predictions have been observed in experiments by adopting suitable strategies to satisfy the rigorous condition of near-degenerate atomic levels and nonorthogonal dipole moments [58–61]. In particular, we consider a three-level Λ configuration in the EIT regime with an extra incoherent pump applied to generate nonvanishing SGC between the two ground levels. Driven into this level configuration, the atomic sample under consideration is found to exhibit gain-assisted double PBGs on the probe transition, benefiting especially from the SGC

*jhwu@nenu.edu.cn

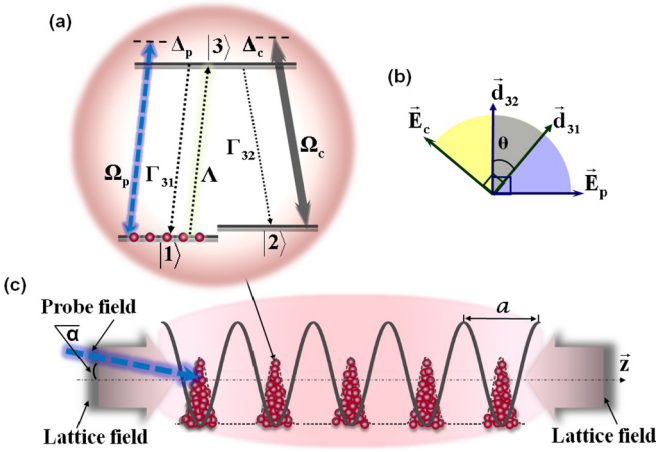

FIG. 1. (a) Schematic of a three-level atomic system driven by a weak probe field of Rabi frequency Ω_p, a strong control field of Rabi frequency Ω_c, and a weak incoherent field of pumping rate Λ. (b) Nonorthogonal arrangement of field polarizations and dipole moments in the probe $|3\rangle \leftrightarrow |1\rangle$ and control $|3\rangle \leftrightarrow |2\rangle$ transitions. (c) Density distribution of cold atoms in periodic traps of a one-dimensional optical lattice with the probe field applied close to the lattice axis.

effect. Such PBGs with reflectivities over 100% and nearby allowed bands with transmissivities over 100% can be easily tuned by modulating the amplitude, frequency, and phase of a strong control field. Exploiting the tunable PBGs and allowed bands as well as their intersecting edges, it is viable to *realize* a reflector, an amplifier, or a splitter as well as to *switch* [48] between them on demand for weak light signals in all-optical networks.

II. MODEL AND EQUATIONS

We start by considering in Fig. 1(a) a three-level Λ system of cold atoms driven by a strong control field of amplitude $\mathbf{E}_c$ and frequency ω_c on transition $|3\rangle \leftrightarrow |2\rangle$ and a weak probe field of amplitude $\mathbf{E}_p$ and frequency ω_p on transition $|3\rangle \leftrightarrow |1\rangle$. An incoherent field of pumping rate Λ is also applied to transition $|3\rangle \leftrightarrow |1\rangle$ so that SGC can exist between indistinguishable pathways $|3\rangle \rightarrow |1\rangle$ and $|3\rangle \rightarrow |2\rangle$ with a nonvanishing population at level $|3\rangle$ [56]. The existence of SGC also requires that dipole moments $\mathbf{d}_{31}$ and $\mathbf{d}_{32}$ are not orthogonal [49,50,55], with θ denoting their relative angle as shown in Fig. 1(b). Figure 1(c) further shows that these atoms are trapped in an OpL formed by a red-detuned standing-wave field of wavelength $\lambda_l = 2a > \lambda_{31}$, with a being the lattice period and λ_{31} the wavelength in transition $|3\rangle \leftrightarrow |1\rangle$.

Using the electric-dipole and rotating-wave approximations, we obtain the interaction Hamiltonian

$$H_I = -\hbar \begin{bmatrix} 0 & 0 & \Omega_p^* \\ 0 & \Delta_p - \Delta_c & \Omega_c^* \\ \Omega_p & \Omega_c & \Delta_p \end{bmatrix}, \tag{1}$$

with detunings $\Delta_p = \omega_p - \omega_{31}$ and $\Delta_c = \omega_c - \omega_{32}$ as well as Rabi frequencies $\Omega_p = (\mathbf{d}_{31} \cdot \mathbf{E}_p)/2\hbar = e^{-i\phi_p} G_p = e^{-i\phi_p} G_{p0} \sin\theta$ and $\Omega_c = (\mathbf{d}_{32} \cdot \mathbf{E}_c)/2\hbar = e^{-i\phi_c} G_c = e^{-i\phi_c} G_{c0} \sin\theta$. Here ϕ_p (ϕ_c) denotes the phase of *complex* amplitude $\mathbf{E}_p$ ($\mathbf{E}_c$), $\pi/2 - \theta$ is the angle between $\mathbf{E}_p$ ($\mathbf{E}_c$) and $\mathbf{d}_{31}$ ($\mathbf{d}_{32}$), and G_{p0} (G_{c0}) represents the maximal Rabi frequency corresponding to $\theta = 0$.

With the Weisskopf-Wigner theory of spontaneous emission [62], we further obtain from Eq. (1) the motion equations of density matrix elements

$$\begin{aligned}
\partial_t \sigma_{11} &= iG_p\sigma_{31} - iG_p\sigma_{13} + \Gamma_{31}\sigma_{33} - \Lambda\sigma_{11}, \\
\partial_t \sigma_{22} &= iG_c\sigma_{32} - iG_c\sigma_{23} + \Gamma_{32}\sigma_{33}, \\
\partial_t \sigma_{21} &= (i\Delta - \gamma_{21})\sigma_{21} + iG_c\sigma_{31} - iG_p\sigma_{23} + \gamma_s e^{i\Phi}\sigma_{33}, \\
\partial_t \sigma_{31} &= (i\Delta_p - \gamma_{31})\sigma_{31} + iG_c\sigma_{21} + iG_p(\sigma_{11} - \sigma_{33}), \\
\partial_t \sigma_{32} &= (i\Delta_c - \gamma_{32})\sigma_{32} + iG_p\sigma_{12} + iG_c(\sigma_{22} - \sigma_{33})
\end{aligned} \tag{2}$$

constrained by $\sigma_{ij} = \sigma_{ji}^*$ and $\sum \sigma_{ii} = 1$. In Eq. (2) $\Phi = \phi_p - \phi_c$ is the relative phase between probe and control fields, $\Delta = \Delta_p - \Delta_c$ is the two-photon detuning in Raman transition $|2\rangle \leftrightarrow |1\rangle$, and Γ_{ij} is the spontaneous decay rate of atomic population σ_{ii} from level $|i\rangle$ to level $|j\rangle$. We have also defined $\gamma_{32} = (\Gamma_{31} + \Gamma_{32})/2$, $\gamma_{31} = (\Gamma_{31} + \Gamma_{32} + \Lambda)/2$, and $\gamma_{21} = \Lambda/2$ as the dephasing rates of atomic coherences σ_{32}, σ_{31}, and σ_{21}, in order. We note, in particular, that an important quantity, $\gamma_s = \frac{|\mathbf{d}_{31}\cdot\mathbf{d}_{32}|}{|\mathbf{d}_{31}||\mathbf{d}_{32}|}\sqrt{\Gamma_{31}\Gamma_{32}}/2 = \cos\theta\sqrt{\Gamma_{31}\Gamma_{32}}/2$, exists in Eq. (2) and will disappear in the case of orthogonal dipole moments ($\theta = \pi/2$) [63]. This is, in fact, a coefficient representing the SGC effect, i.e., the cross-coupling between spontaneous decay pathways $|3\rangle \rightarrow |1\rangle$ and $|3\rangle \rightarrow |2\rangle$.

In the weak probe limit, steady-state solutions for σ_{ij} to all orders of G_c but to zero order of G_p are given by

$$\begin{aligned}
\sigma_{11}^{(0)} &= \frac{\Gamma_{31}(\Gamma_{32} + \Gamma_{31})G_c^2}{(\Gamma_{32} + \Gamma_{31})(2\Lambda + \Gamma_{31})G_c^2 + \Lambda\Gamma_{32}\left[(\Gamma_{32} + \Gamma_{31})^2/4 + \Delta_c^2\right]}, \\
\sigma_{22}^{(0)} &= \frac{\Lambda(\Gamma_{32} + \Gamma_{31})G_c^2 + \Lambda\Gamma_{32}\left[(\Gamma_{32} + \Gamma_{31})^2/4 + \Delta_c^2\right]}{(\Gamma_{32} + \Gamma_{31})(2\Lambda + \Gamma_{31})G_c^2 + \Lambda\Gamma_{32}\left[(\Gamma_{32} + \Gamma_{31})^2/4 + \Delta_c^2\right]}, \\
\sigma_{33}^{(0)} &= \frac{\Lambda(\Gamma_{32} + \Gamma_{31})G_c^2}{(\Gamma_{32} + \Gamma_{31})(2\Lambda + \Gamma_{31})G_c^2 + \Lambda\Gamma_{32}\left[(\Gamma_{32} + \Gamma_{31})^2/4 + \Delta_c^2\right]}, \\
\sigma_{21}^{(0)} &= \frac{\gamma_s e^{i\Phi}(\Gamma_{32} + \Gamma_{31} + \Lambda)\sigma_{33}^{(0)}}{(\Gamma_{32} + \Gamma_{31} + \Lambda)(\Lambda/2 + i\Delta_c) + 2G_c^2},
\end{aligned}$$

$$\sigma_{31}^{(0)} = \frac{2i\gamma_s e^{i\Phi} G_c \sigma_{33}^{(0)}}{(\Gamma_{32}+\Gamma_{31}+\Lambda)(\Lambda/2+i\Delta_c)+2G_c^2},$$
$$\sigma_{32}^{(0)} = \frac{\Lambda\Gamma_{32} G_c[i(\Gamma_{32}+\Gamma_{31})/2-\Delta_c]}{(\Gamma_{32}+\Gamma_{31})(2\Lambda+\Gamma_{31})G_c^2+\Lambda\Gamma_{32}\left[(\Gamma_{32}+\Gamma_{31})^2/4+\Delta_c^2\right]}. \quad (3)$$

Then steady-state solutions for σ_{33} and σ_{31} to all orders of G_c but to first order of G_p can be derived as

$$\sigma_{33}^{(1)} = \sigma_{33}^{(0)} + \frac{iG_cG_p\left\{-\Delta_c\Lambda\left(\sigma_{21}^{(0)}-\sigma_{12}^{(0)}\right)+(\Gamma_{32}+\Gamma_{31})\left[G_c\left(\sigma_{13}^{(0)}-\sigma_{31}^{(0)}\right)-i\Lambda\left(\sigma_{21}^{(0)}+\sigma_{12}^{(0)}\right)/2\right]\right\}}{(\Gamma_{32}+\Gamma_{31})(2\Lambda+\Gamma_{31})G_c^2+\Lambda\Gamma_{32}\left[(\Gamma_{32}+\Gamma_{31})^2/4+\Delta_c^2\right]},$$
$$\sigma_{31}^{(1)} = \frac{-2iG_p\left[(\Lambda+2i\Delta_c-2i\Delta_p)\left(\sigma_{33}^{(0)}-\sigma_{11}^{(0)}\right)+2iG_c\sigma_{32}^{(0)}\right]+4i\gamma_s e^{i\Phi}G_c\sigma_{33}^{(1)}}{(\Gamma_{32}+\Gamma_{31}+\Lambda-2i\Delta_p)(\Lambda+2i\Delta_c-2i\Delta_p)+4G_c^2}. \quad (4)$$

Finally, we write the *complex* probe susceptibility

$$\chi_p(z) = \frac{D(z)|\mathbf{d}_{13}|^2}{2\varepsilon_0\hbar}\frac{\sigma_{31}^{(1)}}{G_p}, \quad (5)$$

with $D(z)$ being the space-dependent atomic density. For cold atoms trapped in an OpL as shown in Fig. 1(c), we may assume identical Gaussian distributions $D(z) = D_0\exp[-(z-z_i)^2/dz^2]$ in each dipole trap with width dz much smaller than period a [64]. It is then convenient to attain the *complex* refractive index $n_p(z) = \sqrt{1+\chi_p(z)}$ whose imaginary and real parts govern, respectively, local probe absorption and dispersive properties. Considering that $n_p(z)$ is periodic along the lattice axis, PBGs are expected to open up near the probe resonance when the Bragg condition $2a = \lambda_{31}/\cos\alpha$ is fulfilled by modulating angle α between the probe field and the lattice axis. This expectation is usually verified by examining the Bloch wave vector and the probe reflectivity, e.g., via the transfer-matrix method as given below.

Starting with $n_p(z)$, we first evaluate a 2×2 unimodular transfer matrix M_j describing the dynamic propagation of a probe field through the jth period of the OpL as detailed in Refs. [65–68]. This matrix satisfies

$$\begin{bmatrix}E_p^+(x+a)\\E_p^-(x+a)\end{bmatrix} = M_j\begin{bmatrix}E_p^+(z)\\E_p^-(z)\end{bmatrix} = \begin{bmatrix}e^{i\kappa a}E_p^+(z)\\e^{i\kappa a}E_p^-(z)\end{bmatrix}, \quad (6)$$

with E_p^+ (E_p^-) being the forward (backward) probe field and κ the Bloch wave vector according to the Bloch theorem. Solution of the determinantal equation $e^{2i\kappa a} - \mathrm{Tr}(M)e^{i\kappa a} + 1 = 0$ restricted by $\det M = 1$ then allows us to examine the photonic band structure near the first Brillouin-zone boundary $\kappa = \pi/a$. One PBG is said to open up if a sudden jump of $\mathrm{Re}(\kappa)$ occurs when the probe detuning Δ_p is modulated near resonance.

Because κ is not accessible in experiments, it will be better to consider other quantities also characterizing the generation of PBGs. As we know, a forward light field may experience multiple Bragg scattering when it propagates through a multilayer structure, which then yields a backward light field. This is especially true when the probe field has carrier frequencies near a PBG. Thus we can examine reflectivity and transmissivity,

$$\mathtt{R} = |r(\Delta_p)|^2 = \left|\frac{M_{(12)}(\Delta_p)}{M_{(22)}(\Delta_p)}\right|^2,$$
$$\mathtt{T} = |t(\Delta_p)|^2 = \left|\frac{1}{M_{(22)}(\Delta_p)}\right|^2, \quad (7)$$

to see whether PBGs open up for a probe field of suitable frequency. In deriving Eq. (7), we have assumed that the sample has N periods so that the total transfer matrix can be expressed as $M = M_1\ldots M_j\ldots M_N$, with $M_{(11)}$, $M_{(12)}$, $M_{(21)}$, and $M_{(22)}$ being four elements.

In realistic situations it is narrow-band light pulses but not monochromatic light fields that are taken as signals in communication networks. Therefore we further use the Fourier transform method to attain expressions describing the propagation dynamics of a probe pulse considering that $r(\Delta_p)$ and $t(\Delta_p)$ will provide all the required information in the linear response regime. The basic procedure is [13,68] (i) to decompose the incident pulse in the time domain $E_{It}(t)$ into the Fourier components in the frequency domain $E_{If}(\Delta_p)$; (ii) to obtain the reflected and transmitted Fourier components $E_{Rf}(\Delta_p) = E_{If}(\Delta_p)\cdot r(\Delta_p)$ and $E_{Tf}(\Delta_p) = E_{If}(\Delta_p)\cdot t(\Delta_p)$; (iii) to make the inverse Fourier transform so that the reflected pulse $E_{Rt}(t)$ at $z=0$ and the transmitted pulse $E_{Tt}(t)$ at $z=L$ can be reconstructed as

$$E_{Rt}(t) = \int E_{Rf}(\Delta_p)e^{-i(\Delta_p-\Delta_0)t}d\Delta_p,$$
$$E_{Tt}(t) = \int E_{Tf}(\Delta_p)e^{-i(\Delta_p-\Delta_0)t}d\Delta_p. \quad (8)$$

For simplicity without loss of generality, we assume that the incident pulse has a Gaussian profile, $E_{It}(t) = E_{0t}e^{-(t-t_0)^2/\tau^2}$ and $E_{If}(\Delta_p) = E_{0f}e^{-(\Delta_p-\Delta_0)^2/\delta_p^2}$, in the time and frequency domains, respectively. Here t_0 and τ (Δ_0 and δ_p) are the center and the width of the incident pulse in the time (frequency) domain.

III. GAIN-ASSISTED PBGs

In this section, we solve Eq. (7) to examine the steady response for a monochromatic probe field near a pair of dynamically induced PBGs. We first consider the case of $\Lambda = 0$ where the incoherent pump is turned off. It is easy to find from Eq. (3)–Eq. (5) that the probe susceptibility χ_p is independent of the SGC coefficient γ_s because we have $\sigma_{33}^{(1)} = \sigma_{33}^{(0)} = 0$ so that SGC cannot occur in the absence of spontaneous decay from state $|3\rangle$. When such a γ_s-independent χ_p is used to calculate R and T in Eq. (7), we can observe in Fig. 2 two PBGs of high reflectivity (~80%) and three allowed bands of high transmissivity (~95%) as a mixed result of EIT and multiple Bragg scattering. They can be easily modulated in width and position around the probe resonance by changing

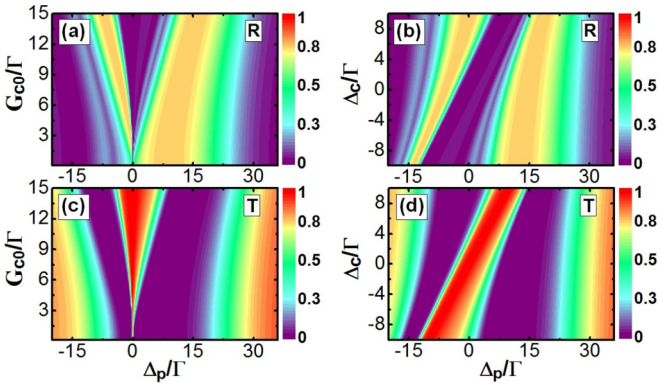

FIG. 2. (a) Reflectivity and (c) transmissivity vs Δ_p and G_{c0} with $\Delta_c = 0$; (b) reflectivity and (d) transmissivity vs Δ_p and Δ_c with $G_{c0} = 13\Gamma$ in the absence of an incoherent pump ($\Lambda = 0$). Other parameters are $G_{p0} = 0.015\Gamma$, $\theta = \pi/4$, $\Gamma_{31} = \Gamma_{32} = 6$ MHz, $d_{13} = d_{23} = 1.0 \times 10^{-29}$ C · m, $D_0 = 5.0 \times 10^{11}$ cm^{-3}, $L = 4$ mm, $\alpha = 0.2^\circ$, and $dz = a/5$.

the Rabi frequency G_{c0} and detuning Δ_c. But their heights are always smaller than 100%, indicating that no optical gain occurs in the absence of an incoherent pump.

Then we consider the case of $\Lambda \neq 0$ to include the incoherent pump. In this case, both $\sigma_{33}^{(1)}$ and χ_p depend critically on the SGC coefficient γ_s. Keep in mind, however, that Λ should be kept very small to ensure that most populations are at level $|1\rangle$ and few atoms escape from level $|3\rangle$ out of the dipole traps. In fact, $\Lambda \leqslant 0.01\Gamma$ with $\Gamma_{31} = \Gamma_{32} = \Gamma$ is low enough to guarantee $\sigma_{33}^{(1)} \lesssim 0.001$. Figures 3(a) and 3(d) show that the absorption coefficient $\mathrm{Im}(\chi_p)$ becomes sensitive to the relative phase Φ when we set $\Lambda = 0.002\Gamma$. In particular, when Φ is increased from 0 to π, (i) $\mathrm{Im}(\chi_p)$ at $\Delta_p \simeq 0$ continuously decreases and gain without inversion occurs for $\Phi > \pi/2$; and (ii) $\mathrm{Im}(\chi_p)$ at $\Delta_p \simeq 20\Gamma$ continuously increases but no gain occurs for any values of Φ. We stress here that the curve for $\Lambda = 0$ and that for $\Lambda = 0.002\Gamma$ and $\Phi = \pi/2$ are

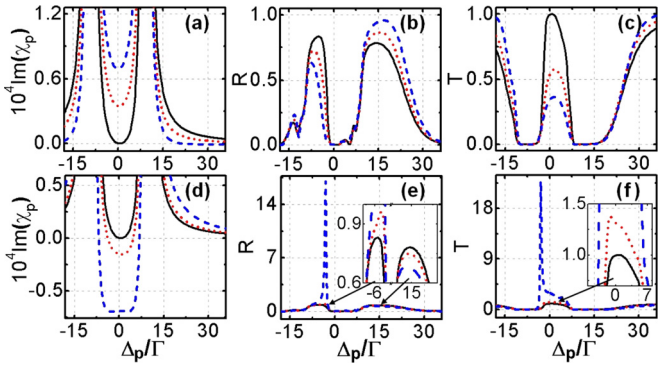

FIG. 3. Imaginary part of the (a) probe susceptibility, (b) reflectivity, and (c) transmissivity vs Δ_p with $\Phi = 0$ (dashed blue line), $\Phi = \pi/3$ (dotted red line), and $\Phi = \pi/2$ (solid black line). Imaginary part of the (d) probe susceptibility, (e) reflectivity, and (f) transmissivity vs Δ_p with $\Phi = \pi/2$ (solid black line), $\Phi = 4\pi/7$ (dotted red line), and $\Phi = \pi$ (dashed blue line). Other parameters are the same as for Fig. 2 except $G_{c0} = 13\Gamma$ and $\Delta_c = 0$ in the presence of an incoherent pump ($\Lambda = 0.002\Gamma$).

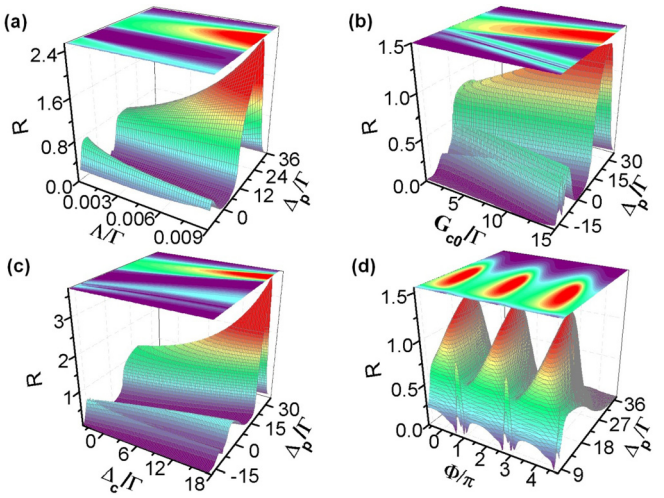

FIG. 4. Reflectivity (a) vs Δ_p and Λ with $\Phi = 0$, $G_{c0} = 13\Gamma$, and $\Delta_c = 0$; (b) vs Δ_p and G_{c0} with $\Lambda = 0.005\Gamma$, $\Phi = 0$, and $\Delta_c = 0$; (c) vs Δ_p and Δ_c with $\Lambda = 0.005\Gamma$, $\Phi = 0$, and $G_{c0} = 13\Gamma$; and (d) vs Δ_p and Φ with $\Lambda = 0.005\Gamma$, $G_{c0} = 13\Gamma$, and $\Delta_c = 0$. Other parameters are the same as for Fig. 2.

almost indistinguishable. In good agreement with Fig. 3(a), Figs. 3(b) and 3(c) show that one could attain a higher probe reflectivity (∼95%) in the right, wide PBG, at the expense of reduced reflectivity (transmissivity) in the left, narrow PBG (the middle allowed band), by decreasing Φ from $\pi/2$ to 0. In good agreement with Fig. 3(d), Figs. 3(e) and 3(f) show that one could attain ∼1100% probe reflectivity (∼1500% transmissivity) in the left, narrow PBG (the middle allowed band), at the expense of reduced reflectivity in the right, wide PBG, by increasing Φ from $\pi/2$ to π. This means that we can realize gain-assisted PBGs characterized by enhanced reflectivities benefiting from the SGC effect in the presence of a very weak incoherent pump. Here an important feature resulting from SGC is that one can modulate the relative phase Φ, in addition to the Rabi frequency G_{c0} and detuning Δ_c, to control the reflectivity and transmissivity.

A more thorough understanding of gain-assisted PBGs might be gained from the surface and contour plots in Fig. 4, where the probe reflectivity is shown for the right, wide PBG. In Fig. 4(a) we can see that it is possible to evidently increase the probe reflectivity without changing the PBG position by using a slightly higher incoherent pump rate Λ. Figures 4(b) and 4(c) show instead that both the reflectivity height and the frequency position of the left PBG can be finely adjusted by manipulating the Rabi frequency G_{c0} and detuning Δ_c of the control field. It is more interesting to note in Fig. 4(d) that the reflectivity height of the right PBG exhibits a sharp periodic pattern as the relative phase Φ is modulated. Similar remarks hold for the left, narrow PBG of a much higher probe reflectivity (not shown). Thus it would be appealing to shape and control photon flows by establishing and manipulating such tunable PBGs with arbitrary gain.

IV. REFLECTOR, AMPLIFIER, AND SPLITTER

In this section, we solve Eq. (8) to examine the dynamic response for a narrow-band probe pulse near a pair of

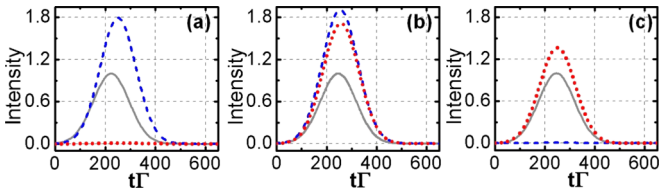

FIG. 5. Scaled intensities of incident, reflected, and transmitted pulses $|E_{It}/E_{0t}|^2$ (solid black line), $|E_{Rt}/E_{0t}|^2$ (dashed blue line), and $|E_{Tt}/E_{0t}|^2$ (dotted red line) vs time t with (a) $\Delta_0 = 16.5\Gamma$, (b) $\Delta_0 = 25\Gamma$, and (c) $\Delta_0 = 40\Gamma$. Other parameters are the same as for Fig. 2 except $\Lambda = 0.009\Gamma$, $G_{c0} = 13\Gamma$, $\Delta_c = 0$, $\Phi = 0$, $t_0 = 235/\Gamma$, and $\tau = 230/\Gamma$.

dynamically induced PBGs. First, we consider in Fig. 5 the case where a Gaussian probe pulse is modulated in frequency to fall into different regions around the right, wide PBG with fixed control Rabi frequency $G_{c0} = 13\Gamma$. We see in Fig. 5(a) that the incident pulse is totally reflected (with a vanishing transmitted signal at $z = L$) in the presence of small gain and negligible deformation when most of its carrier frequencies are inside this PBG. Figure 5(b) shows instead that the incident pulse is reflected and transmitted on a roughly equal footing in the presence of small gain and negligible deformation when its carrier frequencies move right, to be at the the falling (rising) edge of this PBG (an allowed band). The incident pulse may also be totally transmitted (with a vanishing reflected signal at $z = 0$) in the presence of small gain and negligible deformation, as in Fig. 5(c), when most of its carrier frequencies move into this allowed band. These results indicate that our atomic sample can serve as a reflector, a splitter, or an amplifier for narrow-band light signals of distinct center frequencies.

Then we consider in Fig. 6 the case where a Gaussian probe pulse of fixed carrier frequencies falls into the same region around the left, narrow PBG when the Rabi frequency G_{c0} of the control field is modulated. Similar to the results in Fig. 5, once again the incident pulse may experience only reflection [Fig. 6(a)], both reflection and transmission [Fig. 6(b)], or only transmission [Fig. 6(c)], depending on the value of G_{c0}. The reason is that the left, narrow PBG and its neighboring allowed band can be moved by changing G_{c0} to partially or totally cover most carrier frequencies of the incident pulse. Thus, our atomic sample can be engineered to exhibit different functions (reflector, splitter, or amplifier) for manipulating the

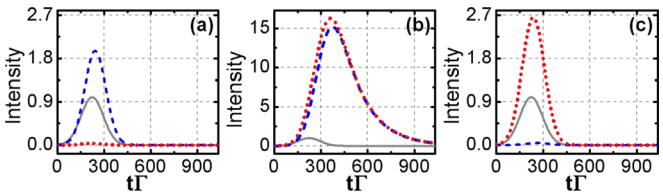

FIG. 6. Scaled intensities of incident, reflected, and transmitted pulses $|E_{It}/E_{0t}|^2$ (solid black line), $|E_{Rt}/E_{0t}|^2$ (dashed blue line), and $|E_{Tt}/E_{0t}|^2$ (dotted red line) vs time t with (a) $G_{c0} = 7.3\Gamma$, (b) $G_{c0} = 10.0\Gamma$, and (c) $G_{c0} = 15.3\Gamma$. Other parameters are the same as for Fig. 2 except $\Lambda = 0.002\Gamma$, $\Delta_0 = -1.95\Gamma$, $\Delta_c = 0$, $\Phi = \pi$, $t_0 = 235/\Gamma$, and $\tau = 230/\Gamma$.

photon flow of a light signal of fixed center frequency. Note, however, that (i) the splitter will yield remarkable deformation for the reflected and transmitted signals in the presence of an ~1500% gain; and (ii) the reflector (amplifier) will not result in obvious deformation for the reflected (transmitted) signal in the presence of an ~190% (~ 260%) gain. This large difference is due to the fact that the left, narrow PBG and its neighboring allowed band have the largest gain in the overlap region [cf. Fig. 3(e) and Fig. 3(f)].

The above discussion therefore results in the expectation of realizing a dynamically controlled multifunctional photonic device. This device might be used either to attain distinct photon flows for three synchronous signals or to attain alterable photon flows for a single signal. The realization needs to adjust the control field in amplitude, frequency, and phase with an incoherent pump applied to activate the SGC effect. The main challenge of our proposal is to have both near-degenerate atomic levels and nonorthogonal dipole moments, a condition rather difficult to find in real systems. To the best of our knowledge, this rigorous condition can be met only in charged quantum dots [58] and ordinary atoms placed near a metallic nanostructure [54] or managed in the dressed-state picture [59]. For the consideration of an experimental realization, near-degenerate levels $|1\rangle$ and $|2\rangle$ in Fig. 1(a) may be regarded as a coherent superposition of two well-separated Zeeman levels $|-\rangle$ and $|+\rangle$ belonging to different hyperfine states, $|5S_{1/2}, F = 1\rangle$ and $|5S_{1/2}, F = 2\rangle$, of ^{87}Rb atoms, exhibiting orthogonal dipole moments $\mathbf{d}_{3-} \perp \mathbf{d}_{3+}$, and coupled by a microwave field of Rabi frequency Ω_m and detuning Δ_m. In this case, we have $|1\rangle = \sin\phi|-\rangle + \cos\phi|+\rangle$ and $|2\rangle = \cos\phi|-\rangle - \sin\phi|+\rangle$ with $\tan\phi = 2\Omega_m/(\sqrt{4\Omega_m^2 + \Delta_m^2} - \Delta_m)$ in the dressed-state picture of this additional microwave field. Then the frequency difference $\omega_{21} = \sqrt{4\Omega_m^2 + \Delta_m^2}$ can be very small and the relative angle $\theta = \arctan[(d_{3+}\tan\phi)/d_{3-}] + \arctan[(d_{3+}/(d_{3-}\tan\phi)]$ can be nonorthogonal. Finally, we stress that our numerical results will not change even if $\theta \neq \pi/4$ as long as $G_c = G_{c0}\sin\theta$ is fixed.

V. CONCLUSIONS

In summary, we have explored SGC activated by a weak incoherent pump to attain gain-assisted double PBGs in a three-level Λ-type EIT system of cold atoms exhibiting a periodic density distribution. We find that both reflectivities in the two PBGs and transmissivities in nearby allowed bands may exceed 100% for a weak probe field and can be adjusted by modulating a strong control field in amplitude and frequency. It is more interesting that the relative phase between probe and control fields also becomes important when it appears along with the SGC coefficient in the expression of probe susceptibility. Then an efficient phase-sensitive reflector, amplifier, or splitter becomes possible when the carrier frequencies of a weak light pulse fall into one PBG, one allowed band, or their intersecting edges. These results are expected to have potential applications in all-optical networks with respect to fabricating dynamically switchable devices for manipulating photon flows at low-light levels. The amplifier function may be exploited to further attain the more appealing transistor function [69] when a weak auxiliary field is introduced to manipulate the probe transmissivity in a slightly extended level configuration.

ACKNOWLEDGMENTS

This work was supported by the National Natural Science Foundation of China (Grants No. 11247005, No. 61378094, and No. 11534002), Fundamental Research Funds for Central Universities of China (Grant No. 12QNJJ006), and the Postdoctoral Scientific Research Program of Jilin Province (Grant No. RB201330).

[1] S. John, Phys. Rev. Lett. **58**, 2486 (1987).
[2] K. Sakoda, *Optical Properties of Photonic Crystals* (Springer, Berlin, 2001).
[3] I. H. Deutsch, R. J. C. Spreeuw, S. L. Rolston, and W. D. Phillips, Phys. Rev. A **52**, 1394 (1995).
[4] A. Andre and M. D. Lukin, Phys. Rev. Lett. **89**, 143602 (2002).
[5] X. Wu, A. Yamilov, X. Liu, S. Li, V. P. Dravid, R. P. H. Chang, and H. Cao, Appl. Phys. Lett. **85**, 3657 (2004).
[6] M. Straub, M. Ventura, and M. Gu, Phys. Rev. Lett. **91**, 043901 (2003).
[7] M. Scharrer, A. Yamilov, X. Wu, H. Cao, and R. P. H. Chang, Appl. Phys. Lett. **88**, 201103 (2006).
[8] K. Ishizaki and S. Noda, Nature **460**, 367 (2009).
[9] M. Greiner and S. Fölling, Nature **453**, 736 (2008).
[10] X.-M. Su and B. S. Ham, Phys. Rev. A **71**, 013821 (2005).
[11] M. Artoni and G. C. La Rocca, Phys. Rev. Lett. **96**, 073905 (2006).
[12] S.-Q. Kuang, R.-G. Wan, P. Du, Y. Jiang, and J.-Y. Gao, Opt. Express **16**, 15455 (2008).
[13] Y. Zhang, Y. Xue, G. Wang, C.-L. Cui, R.-G. Wang, and J.-H. Wu, Opt. Express **19**, 2111 (2011).
[14] D.-W. Wang, H.-T. Zhou, M.-J. Guo, J.-X. Zhang, J. Evers, and S.-Y. Zhu, Phys. Rev. Lett. **110**, 093901 (2013).
[15] J. Wu, Y. Liu, D.-S. Ding, Z.-Y. Zhou, B.-S. Shi, and G. C. Guo, Phys. Rev. A **87**, 013845 (2013).
[16] B. Little, D. J. Starling, J. C. Howell, R. D. Cohen, D. Shwa, and N. Katz, Phys. Rev. A **87**, 043815 (2013).
[17] V. G. Arkhipkin and S. A. Myslivets, Opt. Lett. **39**, 3223 (2014).
[18] D.-W. Wang, S.-Y. Zhu, J. Evers, and M. O. Scully, Phys. Rev. A **91**, 011801(R) (2015).
[19] Y. Zhang, Y.-M. Liu, X.-D. Tian, T.-Y. Zheng, and J.-H. Wu, Phys. Rev. A **91**, 013826 (2015).
[20] S. E. Harris, Phys. Today **50**, 36 (1997).
[21] M. Fleischhauer, A. Imamoglu, and J. P. Marangos, Rev. Mod. Phys. **77**, 633 (2005).
[22] Q.-Q. Bao, X.-H. Zhang, J.-Y. Gao, Y. Zhang, C.-L. Cui, and J.-H. Wu, Phys. Rev. A **84**, 063812 (2011).
[23] H. M. M. Alotaibi and B. C. Sanders, Phys. Rev. A **89**, 021802(R) (2014).
[24] N. Radwell, T. W. Clark, B. Piccirillo, S. M. Barnett, and S. Franke-Arnold, Phys. Rev. Lett. **114**, 123603 (2015).
[25] P. Verkerk, B. Lounis, C. Salomon, C. Cohen-Tannoudji, J.-Y. Courtois, and G. Grynberg, Phys. Rev. Lett. **68**, 3861 (1992).
[26] A. Hemmerich and T. W. Hänsch, Phys. Rev. Lett. **70**, 410 (1993).
[27] P. S. Jessen and I. H. Deutsch, Adv. At. Mol. Opt. Phys. **37**, 95 (1996).
[28] C. R. Rosberg, D. N. Neshev, A. A. Sukhorukov, Y. S. Kivshar, and W. Krolikowski, Opt. Lett. **30**, 2293 (2005).
[29] O. Morsch and M. Oberthaler, Rev. Mod. Phys. **78**, 179 (2006).
[30] I. Bloch, Nature **453**, 1016 (2008).
[31] L. Li, Y. O. Dudin, and A. Kuzmich, Nature **498**, 466 (2013).
[32] M. Pasienski, D. McKay, M. White, and B. DeMarco, Nat. Phys. **6**, 677 (2010).
[33] P. M. Visser and G. Nienhuis, Opt. Commun. **136**, 470 (1997).
[34] G. Birkl, M. Gatzke, I. H. Deutsch, S. L. Rolston, and W. D. Phillips, Phys. Rev. Lett. **75**, 2823 (1995).
[35] M. Weidemüller, A. Hemmerich, A. Görlitz, T. Esslinger, and T. W. Hänsch, Phys. Rev. Lett. **75**, 4583 (1995).
[36] S. Slama, C. von Cube, B. Deh, A. Ludewig, C. Zimmermann, and Ph. W. Courteille, Phys. Rev. Lett. **94**, 193901 (2005).
[37] S. Slama, C. von Cube, M. Kohler, C. Zimmermann, and Ph. W. Courteille, Phys. Rev. A **73**, 023424 (2006).
[38] A. Schilke, C. Zimmermann, P. W. Courteille, and W. Guerin, Phys. Rev. Lett. **106**, 223903 (2011).
[39] M. Antezza and Y. Castin, Phys. Rev. A **80**, 013816 (2009).
[40] D. Yu, Phys. Rev. A **84**, 043833 (2011).
[41] D. Petrosyan, Phys. Rev. A **76**, 053823 (2007).
[42] A. Schilke, C. Zimmermann, and W. Guerin, Phys. Rev. A **86**, 023809 (2012).
[43] H. Yang, L. Yang, X.-C. Wang, C.-L. Cui, Y. Zhang, and J.-H. Wu, Phys. Rev. A **88**, 063832 (2013).
[44] L. Yang, Y. Zhang, X.-B. Yan, Y. Sheng, C.-L. Cui, and J.-H. Wu, Phys. Rev. A **92**, 053859 (2015).
[45] S. A. R. Horsley, J.-H. Wu, M. Artoni, and G. C. La Rocca, Phys. Rev. Lett. **110**, 223602 (2013).
[46] J.-H. Wu, M. Artoni, and G. C. La Rocca, Phys. Rev. Lett. **113**, 123004 (2014).
[47] K. Zhou, T. Wei, H. Sun, Y. He, and S. Liu, Opt. Express **23**, 16903 (2015).
[48] S. M. Sadeghi, W. Li, X. Li, and W.-P. Huang, Phys. Rev. B **73**, 035304 (2006).
[49] J. Javanainen, Europhys. Lett. **17**, 407 (1992).
[50] S. Menon and G. S. Agarwal, Phys. Rev. A **57**, 4014 (1998).
[51] P. R. Berman, Phys. Rev. A **72**, 035801 (2005).
[52] T. Shui, Z. Wang, and B. Yu, J. Opt. Soc. Am. B **32**, 210 (2015).
[53] S.-Y. Zhu and M. O. Scully, Phys. Rev. Lett. **76**, 388 (1996).
[54] V. Yannopapas, E. Paspalakis, and N. V. Vitanov, Phys. Rev. Lett. **103**, 063602 (2009).
[55] Y. Niu and S. Gong, Phys. Rev. A **73**, 053811 (2006).
[56] J.-H. Wu and J.-Y. Gao, Phys. Rev. A **65**, 063807 (2002).
[57] D. Wang and Y. Zheng, Phys. Rev. A **83**, 013810 (2011).
[58] M. V. Dutt, J. Cheng, B. Li, X. Xu, X. Li, P. R. Berman, D. G. Steel, A. S. Bracker, D. Gammon, S. E. Economou, R. B. Liu, and L. J. Sham, Phys. Rev. Lett. **94**, 227403 (2005).
[59] C.-L. Wang, A.-J. Li, X.-Y. Zhou, Z.-H. Kang, J. Yun, and J.-Y. Gao, Opt. Lett. **33**, 687 (2008).
[60] C.-L. Wang, Z.-H. Kang, S.-C. Tian, Y. Jiang, and J.-Y. Gao, Phys. Rev. A **79**, 043810 (2009).
[61] S.-C. Tian, C.-L. Wang, C.-Z. Tong, L.-J. Wang, H.-H. Wang, X.-B. Yang, Z.-H. Kang, and J.-Y. Gao, Opt. Express **20**, 23559 (2012).
[62] M. O. Scully and M. S. Zubairy, *Quantum Optics* (Cambridge University Press, Cambridge, UK, 1997).

[63] P. Zhou and S. Swain, Phys. Rev. Lett. **77**, 3995 (1996).
[64] J.-H. Wu, S. A. R. Horsley, M. Artoni, and G. C. La Rocca, Light: Sci. Appl. **2**, e54 (2013).
[65] M. Born and E. Wolf, *Principles of Optics*, 6th ed. (Cambridge University Press, Cambridge, UK, 1980).
[66] M. Artoni, G. C. La Rocca, and F. Bassani, Phys. Rev. E **72**, 046604 (2005).
[67] Y. Zhang, J.-W. Gao, C.-L. Cui, Y. Jiang, and J.-H. Wu, Phys. Lett. A **374**, 1088 (2010).
[68] J.-H. Wu, G. C. La Rocca, and M. Artoni, Phys. Rev. B **77**, 113106 (2008).
[69] Z.-G. Wang, Z. Ullah, M.-Q. Gao, D. Zhang, Y.-Q. Zhang, H. Gao, and Y.-P. Zhang, Sci. Rep. **5**, 13880 (2015).